CORRELATION OF PP DATA WITH PREDICTIONS OF IMPROVED SIX-QUARK STRUCTURE MODELS*

P. González**, P. LaFrance and E. L. Lomon

Center for Theoretical Physics
Laboratory for Nuclear Science
and Department of Physics
Massachusetts Institute of Technology
Cambridge, Massachusetts 02139 U.S.A.

Submitted to: *Phys. Rev. D*

Typeset in TEX by Roger L. Gilson

CTP# 1383 August 1986

* This work is supported in part by funds provided by the U. S. Department of Energy (D.O.E.) under contract #DE-AC02-76ER03069.

** On leave of absence from Departamento de Física Teórica, Valencia, SPAIN.

CORRELATION OF PP DATA WITH PREDICTGIONS OF IMPROVED SIX-QUARK STRUCTURE MODELS

P. González, P. LaFrance and E. L. Lomon

ABSTRACT*

Recent experimental data has shown a structure in $\Delta\sigma_L$ corresponding to a pp mass of 2.7 GeV/c^2, as earlier predicted for a six-quark $^1S_0$ state by an R-matrix treatment of CBM quark degrees of freedom interior to a coupled isobar channel system. The $^1S_0$ model is improved to agree with 2π production data at 800 MeV laboratory energy. The resulting $^1S_0$ partial wave and recently improved models of the background partial waves as well as older versions of the phase parameter predict experimental observables in the resonance region. The predicted width and inelasticity are consistent with the data. Detailed energy and angular dependence of the model are in agreement with $\Delta\sigma_L$, C_{LL} and C_{NN} data in the resonance energy region. More data on these observables is needed to confirm the structure and its characteristics. Measurable aspects of the structure in other observables are displayed. Another six-quark resonance structure, in the $^1D_2$ state, is described.

I. INTRODUCTION

Recent experimental data[1] shows a new structure in $\Delta\sigma_L$, the difference between proton-proton total cross sections for antiparallel and parallel longitudinally polarized spin states at $P_L = 2.75$ GeV/c. Earlier indications of structure at this laboratory momentum were seen in C_{LL} [2] and C_{NN} [3] measurements near 90°. If the present data is ascribed to a resonance its mass would be about 2.70 GeV/c^2, the width less than 80 MeV and the elasticity greater than 0.1.[1] These characteristics have been predicted[4] to result from a 6-quark state in a model using a Cloudy Bag Model (CBM)[5] dynamics at short range and meson exchange potentials between nucleons and isobars at long range. The R-matrix formalism determines the interior boundary condition on the hadronic wave functions in terms of the interior six-quark states.

In this model, the width, energy splitting and inelastic modes of the resonances (sometimes referred to as dibaryons) are characteristic of general properties of the six-quark states, and their absolute masses are characteristic of the particular quark model used. The amplitude of the structures and the backgrounds are sensitive to the long range hadronic characteristics of the interaction.

* PACS: 12;40A, 13.75C, 14.20.P.

Although the models are largely determined by theory, they have some parameters (described in Section II) which are fixed by comparison with phase shift analyses of the data for laboratory energy $T_L < 1$ GeV. For some of the results we use the models described in Refs. [4]. Because of the sensitivity to details when extrapolating from $T_L = 1$ GeV to $T_L \leq 2$ GeV, we also show the result of (a) using the improved models for the background partial waves of Ref. [6], and (b) a new improved model of the resonant $^1S_0$ phase shift described in Section II. We also extend the methods of Ref. [6] to determine the six-quark structure in the $^1D_2$ state which is predicted to have a mass near 2.88 GeV/c^2 for the CBM dynamics.

As the $^1D_2$ six-quark resonance energy corresponds to extrapolating a further 0.5 GeV in T_L, both the position of the structure and its interference with background partial waves have more uncertainty than for the $^1S_0$ structure. Consequently, we have not attempted detailed prediction of the effect on observables of this structure. However, the amplitudes of the structure in the $^1D_2$ partial wave is shown to be ample to result in measurable effects.

In Section III we investigate the correlations of the predictions of the above choices of $^1S_0$ resonant models with the $\Delta\sigma_L$, C_{LL} and C_{NN} data in the region of the observed resonance. The predicted mass of the resonance is consistent with that indicated by the data, but may be up to 25 MeV/c^2 lower. The predicted width and inelasticity are consistent with the data. We find many similarities of detailed energy and angular dependence, if one allows for small shifts of angle and some disagreement with background values of the observables. The comparison shows that more precise data at lower energy intervals is needed to establish a structure and to show positively that its characteristics are the ones required by the six-quark state.

In Section III we also show the predicted structure in several other observables which presently have little or no data in the resonance energy region. Section IV draws conclusions and indicated future directions for experimental verification and model improvements.

II. THE MODEL FOR THE $^1S_0$ AND $^1D_2$ CHANNELS

The application of the R-matrix method, in its f-matrix form, to the study of nucleon-nucleon scattering has been described elsewhere.[4,6,7] Briefly, space is divided into two regions in which different approximate forms of the Hamiltonian are applicable. In terms of the nucleon-nucleon relative coordinate, r, there is a boundary (or separation) radius r_0. For $r > r_0$ the interaction is given by a meson exchange potential-matrix between nucleons and isobars. For $r < r_0$ a model incorporating the short range asymptotic freedom of quarks and gluons (such as various "bag" or "constituent quark" models) is used. The energy dependence of the boundary condition on the external wavefunction at r_0 is determined by a complete set of interior six-quark states. When the interior states are characterized by vanishing wavefunctions at r_0 (which seems appropriate in connection with the confinement features of QCD) then the boundary condition is on the logarithmic derivative of the wavefunction, stated in terms of the f-matrix

$$r_0 \frac{d\psi_\alpha^W}{dr_0} = \sum_\beta f_{\alpha\beta} \psi_\beta^W(r_0) \tag{1}$$

with

$$f_{\alpha\beta} = f^0_{\alpha\beta} + \sum_i \frac{\rho^i_{\alpha\beta}}{W - W_i} \tag{2}$$

where the W_i are the energies of the internal six-quark states and

$$\rho^i_{\alpha\beta} = -r_0 \frac{\partial W_i}{\partial r_0} \xi^i_\alpha \xi^i_\beta \tag{3}$$

the ξ^i_α being the fractional percentage coefficient of channel α to the internal state i. Only the constant terms $f^0_{\alpha\beta}$ are completely free parameters.

The value of r_0 is constrained by the requirements of asymptotic freedom in the interior, and adequate clustering into hadrons, due to the onset of confinement, in the exterior. This implies[4] that

$$0.8\, r_{eq} < r_0 < r_{eq} \quad . \tag{4}$$

where r_{eq} is the internucleon distance for the equilibrium radius of the particular quark model. Fitting the nucleon-nucleon scattering data for $T_L < 1$ GeV determines whether an r_0 in the above range is allowable and, if so, fine tunes the value.

With respect to the exterior interaction, the nucleon-nucleon sector of the potential matrix is given by the Feshbach-Lomon interaction,[8] which is determined by π-, η-, ρ- and ω-meson exchange and two-pion exchange contributions (the non-relativistic nature of the two-pion contribution introduces two parameters which were completely determined[8] by the data for $T_L < 400$ MeV). For the transition potentials from the two-nucleon sector to the sector containing isobars, only the one-pion exchange part is taken from theory. The contribution of two-pion and heavier meson exchange is ignored or put in as a two-pion range Yukawa potential of parameterized strength.

A. THE $^1S_0$ NUCLEON-NUCLEON STATE

The $^1S_0$ analyses of Refs. [4] and [7] have been revised with the improved formalism of Ref. [6] (which introduces the isobar widths by distributing isobar masses over many channels). In addition, we now take into account the two-pion production data[9] at $T_L = 0.8$ GeV, which being small, severly limits the coupling to the S-wave $\Delta\Delta$ and $NN^*(1440)$ channels.[10] Consequently, in order to maintain a fit to the $\delta(^1S_0)$ energy dependence, coupling strength has to be shifted (via the constant terms in the f-matrix) to the $N\Delta(^5D_0)$ state. This in turn increases the inelasticity near $T_L = 800$ MeV. The fits shown in Fig. 1 (for values of r_0 corresponding to the Feshbach-Lomon interaction,[7,8] $r_0^{\rm FL} = 0.75$ fm and to the CBM interior,[4] $r_0^{\rm CBM} = 1.05$ fm) assume that about one-half of the two-pion production at $T_L = 0.8$ GeV comes from the $^1S_0$ partial wave. As shown, the resulting $\eta(^1S_0)$ is smaller than that of the phase shift analysis[11,12] near 0.8 GeV, especially for the $r_0^{\rm CBM}$ case. This situation could be improved by coupling to isobar channels with higher energy thresholds, by data indicating that nearly all of the two-pion production comes from the $^1S_0$ channel or by changes in the phase shift analysis. However, the larger deviation for the CBM case indicates that this case may have too large a value of r_0. There are similar indications in the fitting of the $^3S_1 - {}^3D_1$ channel.[4] Therefore, the CBM dynamics may need some modification for complete consistency with two-nucleon data. We note that the addition to the CBM

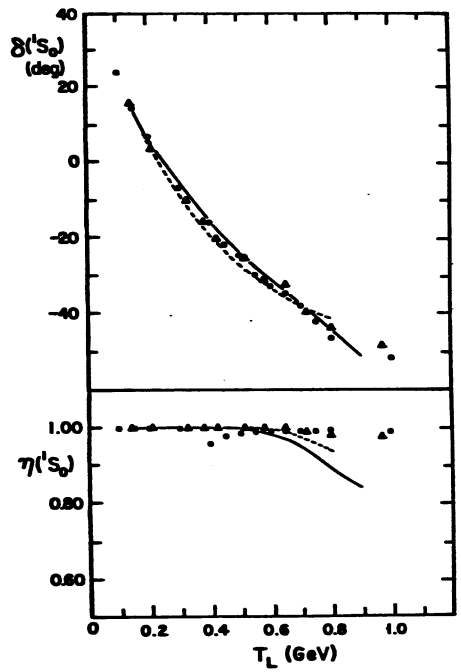

Fig. 1: The $^1S_0$ phase parameters. The open triangles denote the phase shift analysis of Ref. [11], and the open circles that of Ref. [12]. The curves are model predictions for $NN(^1S_0)$ coupled to $N\Delta(^5D_0)$, $NN^*(^1S_0)$ and $\Delta\Delta(^1S_0)$. The solid line represents the CBM dynamics with $r_0^{\rm CBM} = 1.05$ fm and $W_p = 2.71$ GeV. The f-matrix elements are $f_{NN,NN} = 34.78$, $f_{N\Delta,N\Delta} = 5.0$, $f_{NN^*,NN^*} = 2.4$, $f_{\Delta\Delta,\Delta\Delta} = 3.0$, $f_{NN,N\Delta} = -14.33$, $f_{NN,\Delta\Delta} = 6.5$ and $f_{NN,NN^*} = f_{N\Delta,NN^*} = f_{N\Delta,\Delta\Delta} = 0.0$. The dashed line corresponds to $r_0^{\rm FL}$ boundary radius, and the f-pole set by CBM dynamics at $W_p = 3.445$ GeV has a small, almost constant effect over the whole range of energies considered. The potential matrix is common to both cases and is described in the text.

of a small, attractive quark self-energy would decrease r_0 while making little change in the energy of the lowest states (as an increase in kinetic energy is countered by a decrease in potential energy).

For the CBM case, as shown in Refs. [4], the f-pole is consistent with the data and Eq. (4) at $r_0 = 1.05$ fm at a barycentric mass of 2.71 GeV/c^2 (corresponding to $T_l = 2.04$ GeV and $P_L = 2.82$ GeV/c). The pole residues, as determined by the

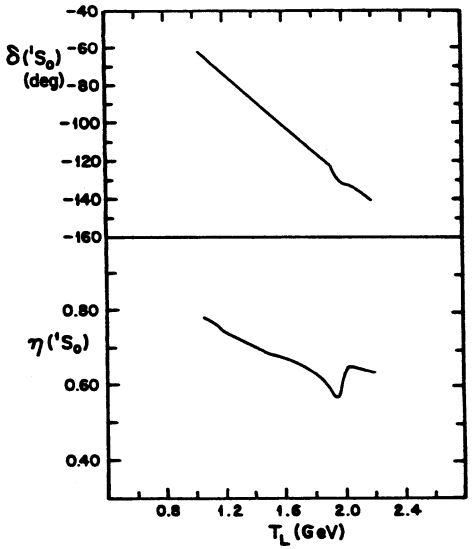

Fig. 2: The higher energy $^1S_0$ phase parameters for the CBM dynamics. The model parameters are as in Fig. 1.

non-vanishing fractional parentage coefficients in the $NN(^1S_0)$, $\Delta\Delta(^1S_0)$ sector,[4] are $\rho_{NN,NN} = 0.149$ GeV, $\rho_{NN,\Delta\Delta} = 0.133$ GeV and $\rho_{\Delta\Delta,\Delta\Delta} = 0.118718$ GeV. The constant terms in the f-matrix are given in the caption to Fig. 1. The transition potentials for this case, as for the $r_0^{\rm FL}$ case are

$$V_{NN,N\Delta} = 0.22\left(1 + \frac{3}{\mu r} + \frac{3}{(\mu r)^2}\right)\frac{e^{-\mu r}}{r}$$

$$V_{NN,\Delta\Delta} = 0.172\,\frac{e^{-\mu r}}{r}$$

and

$$V_{NN,NN^*} = -0.034\,\frac{e^{-\mu r}}{r}$$

with no phenomenological two-pion range potentials.

The extrapolation of the $^1S_0$ CBM model to the six-quark resonance region is shown in Fig. 2. Small dips in η are present at the NN^* and $\Delta\Delta$ thresholds. A knee in $\delta(^1S_0)$ and a dip-bump structure in $\eta(^1S_0)$ are seen to be centered just below

the six-quark state energy. (There is a shift in the pole of $f_{\rm eff}(^1S_0)$ due to channel coupling, as described in Refs. [4] for the $^1S_0$ channel and discussed below for the $^1D_2$ channel.) The width of the structure is about 50 MeV/c^2 in barycentric mass. The value of $\eta^2 > 0.3$ is consistent with the elasticity of the experimental structure,[1] which is > 0.1. Note that the actual change due to the resonance is $\Delta\eta^2 = 0.1$, the rest of the inelasticity being due to the background. The amplitude of the structure in both $\delta(^1S_0)$ and $\eta(^1S_0)$ is about half that of that of Refs. [4].

We will use both the present model (which we will designate NS) and that of Refs. [4] (designated by OS) to predict the pp observables. The OS predicts much too large two-pion production at $T_L = 0.8$ GeV; nevertheless, it may predict the $^1S_0$ amplitude at $T_L = 2$ GeV better than NS. The reason is that the decreased coupling to the $\Delta\Delta$ and NN^* channels in NS causes an increase at high energy in the background $f_{\rm eff}$ in the $NN(^1S_0)$ channel.[4,6,7] This increase may well be cancelled by contributions from higher energy isobar thresholds that do not contribute substantially to the two-pion production at $T_L = 0.8$ GeV, but all of which decrease $f_{\rm eff}$. The larger $f_{\rm eff}$ act as a repulsive core, decreasing the coupling to the interior six-quark states and decreasing the amplitudes of the inelastic resonance.

B. THE $^1D_2$ NUCLEON-NUCLEON STATE

A new fit to the $^1D_2$ phase shift and inelasticity for $r_0^{\rm FL}$ was presented in Ref. [6]. This fit properly includes transition potentials and isobar width effects. It also includes the $N\Delta(^5D_2)$ channel in addition to the $N\Delta(^5S_2)$ channel of Ref. [7], and fits newer phase shift analyses.

We now include the internal CBM dynamics, increasing the value of r_0 and introducing a pole into the f-matrix. The $I = 0$, $J^P = 2^+$ $(^1S_{1/2})^6$ quark configuration has $N\Delta(^5S_2)$ and $\Delta\Delta(^5S_2)$ color-singlet-pair components $[\xi^2_{N\Delta}(^5S_2) = \frac{1}{6}$ and $\xi^2_{\Delta\Delta}(^5S_2) = \frac{1}{30}.]$ [13] The rest of the configuration is "hidden color".

Note that the six-quark state has no $NN(^1D_2)$ component and that consequently the effect of the f-pole does not come directly into the NN sector. However, the construction of $f_{\rm eff}$ $(^1D_2)$ for this chain of coupling[14] $NN(^1D_2) \leftrightarrow N\Delta(^5S_2) \leftrightarrow \Delta\Delta(^5S_2)$ shows that the pole structure is transmitted to the nucleon-nucleon state. For simplicity, we describe the analytic result in the approximation that we neglect the transition potentials and all coupling to the $N\Delta(^5D_2)$ channel. We also use the fact that direct boundary coupling of the NN to the $\Delta\Delta$ channel is absent in the fitted model described below. Then, as shown in Ref. [14] (the notation assumes that the NN channel is $^1D_2$ and that the $N\Delta$ and $\Delta\Delta$ channels are $^5S_2$)

$$f^{NN}_{\rm eff} = f_{NN,NN} - \frac{f^2_{NN,N\Delta}}{f_{N\Delta,N\Delta} - f^2_{N\Delta,\Delta\Delta}\left(f_{\Delta\Delta,\Delta\Delta} + \theta^+_{\Delta\Delta}\right)^{-1} + \theta^+_{N\Delta}} \tag{5}$$

where the θ^+ functions[4,7,14] are the logarithmic derivative of the outgoing wavefunctions in the designated channels. Using $f_{NN,NN} = f^0_{NN,NN}$ and that for the $N\Delta$ and $\Delta\Delta$ channels $f_{ij} = f^0_{ij} + \rho_{ij}(W - W_p)^{-1}$, we get, after performing some algebra and using $\rho_{ij} = \sqrt{\rho_{ii}\rho_{jj}}$,

$$f^{NN}_{\rm eff} = f^0_{NN,NN} + \rho_{\rm eff}(W - W_{\rm eff})^{-1} \tag{6}$$

where

$$W_{\rm eff} = W_p - D^{-1}\left[\rho_{\Delta\Delta,\Delta\Delta}\left(f^0_{N\Delta,N\Delta} + \theta^+_{N\Delta}\right) + \rho_{N\Delta,N\Delta}\left(f^0_{\Delta\Delta,\Delta\Delta} + \theta^+_{\Delta\Delta}\right)\right] \tag{7}$$

and

$$\rho_{\rm eff} = D^{-2}\left(f^0_{NN,N\Delta}\right)^2\left[\rho^{1/2}_{N\Delta,N\Delta}\left(f^0_{\Delta\Delta,\Delta\Delta} + \theta^+_{\Delta\Delta}\right) - \rho^{1/2}_{\Delta\Delta,\Delta\Delta} f^0_{N\Delta,\Delta\Delta}\right]^2 \tag{8}$$

where

$$D = \left(f^0_{N\Delta,N\Delta} + \theta^+_{N\Delta}\right)\left(f^0_{\Delta\Delta,\Delta\Delta} + \theta^+_{\Delta\Delta}\right) - \left(f^0_{N\Delta,\Delta\Delta}\right)^2 \tag{9}$$

Eqs. (8) and (9) show that the residue is positive when $\theta^+_{\Delta\Delta}$ and $\theta^+_{N\Delta}$ are real, so that $df_{\rm eff}/dW < 0$ below inelastic threshold as required. We also note that when $f^0_{N\Delta,\Delta\Delta} = 0$, as in our present fit, Eqs. (8) and (9) are greatly simplified and consequently

$$\begin{aligned} W_{\rm eff}\left(f^0_{N\Delta,\Delta\Delta} = 0\right) = W_p &- \rho_{\Delta\Delta,\Delta\Delta}\left(f^0_{\Delta\Delta,\Delta\Delta} + \theta^+_{\Delta\Delta}\right)^{-1} \\ &- \rho_{N\Delta,N\Delta}\left(f^0_{N\Delta,N\Delta} + \theta^+_{N\Delta}\right)^{-1} \end{aligned} \tag{7'}$$

and

$$\rho_{\rm eff} = \left(f^0_{NN,N\Delta}\right)^2 \rho_{N\Delta,N\Delta}\left(f^0_{N\Delta,N\Delta} + \theta^+_{N\Delta}\right)^{-2} \tag{8'}$$

Eq. (7′) shows that $\mathrm{Re}\, W_{\rm eff}$ is shifted downwards slightly from W_p.

We note that the pure pole dependence of the f-matrix components is modified in $f_{\rm eff}$ by the analytic structure of the θ^+ functions, which, however, have little dependence in the resonance region.

As in Refs. [4], the value of r_0 is determined by the cross-over of the six-quark state energy and the (extrapolated) f-pole energy curves as a function of r. Figure 3 shows the mass curves for both the MIT and Cloudy Bag Models. The f-pole curve is based on the phase shift analysis[12] up to $T_L = 0.8$ GeV. For the MIT Bag Model, it is seen that $r_0 > r_{eq}$ in contradiction with our requirements, Eq. (4). As it is for the $^1S_0$ and $^3S_1$ states, the MIT Bag Model is inconsistent with the $T_L < 1$ GeV data.[4] For the CBM, consistency with Eq. (4) is clearly possible. Unfortunately, given the large extrapolation needed, the whole range of Eq. (4) is consistent. The $r_0^{\rm CBM} = 1.05$ fm for the $^1S_0$ state is at the lower end of the range. For our present predictions, we choose this value for simplicity, and also because the data, as for the $^1S_0$ and $^3S_1$ cases, is better fitted with a smaller radius. This choice of r_0 predicts an f-pole at 2.88 GeV/c^2 (corresponding to $T_L = 2.54$ GeV), and $\rho_{N\Delta,N\Delta} = 0.26$ GeV, $\rho_{N\Delta,\Delta\Delta} = 0.1163$ GeV and $\rho_{\Delta\Delta,\Delta\Delta} = 0.052$ GeV. The effect of increasing r_0 to 0.9 r_{eq} would be to shift the pole to 2.74 GeV/c^2 and to decrease the residues (and consequently the predicted width) by a factor of two.

The fit to $\delta(^1D_2)$ and $\eta(^1D_2)$ for $T_L < 0.8$ GeV is not visibly different from that shown in Fig. 1 of Ref. [6], for $r_0 = r_0^{\rm FL}$, and we do not reproduce it here. But, we remind the reader that the $^1D_2$ resonance at $T_L = 0.6$ GeV is well-reproduced by the effect of the $N\Delta$ threshold. The potential matrix is given in Ref. [6], including the fitted $V_{2\pi}$ coefficients. The constant part of the f-matrix is given in the caption to Fig.

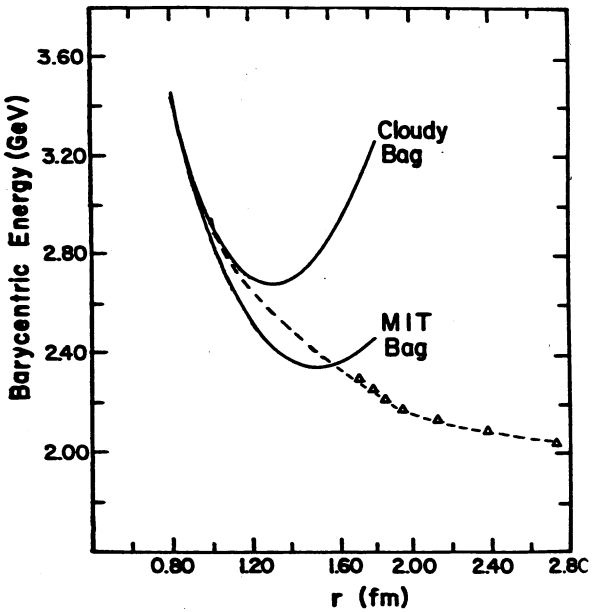

Fig. 3: Quark model masses and experimental f-matrix poles. The solid curves are the barycentric energies of the MIT Bag and Cloudy Bag Model dynamics with quarks confined at $R = 0.88\,r$ (r is the internucleon distance). The triangles represent the f-matrix pole energy at each r derived from the experimental $^1S_0$ phase parameters[12] and the potential matrix described in the text. The dashed line is our chosen extrapolation of the f-pole curve.

4 which shows the extrapolation of the fit to $T_L = 3.2$ GeV. The six-quark resonance produces a small knee in $\delta(^1D_2)$ and a substantial peak in $\eta(^1D_2)$ centered just below $T_L = 2.54$ GeV, with a width of about 100 MeV. The width is larger than for the $^1S_0$ case because $\xi^2_{N\Delta,N\Delta}(^1D_2) = 1.5\xi^2_{\Delta\Delta,\Delta\Delta}(^1S_0)$ and because $\frac{\partial W}{\partial r_0}$ is larger due to the higher energy of the 2^+ quark configuration. The amplitude of the pole effect in δ and η is about half that in the $^1S_0$ case. The structure is about half inelastic as $\eta(^1D_2) = 0.7$ at the resonance peak. Figure 5 shows that the $^1D_2$ contribution to $N\Delta$ production has a dip at the resonance. We note that the $^1D_2$ structure is predicted to be about 170 MeV/c^2 above the $^1S_0$ structure for our present choice of $r_0 = 0.8\,r_{eq}$, but that it would be only about 30 MeV/c^2 higher if $r_0 = 0.9\,r_{eq}$. As for the S-wave six-quark resonances,[4] the dominance of the interior free-quark wave functions at the resonance is shown in Fig. 6.

We can therefore expect that experimental observables will exhibit structures at the $^1D_2$ six-quark pole of about twice the width and half the amplitude of those due

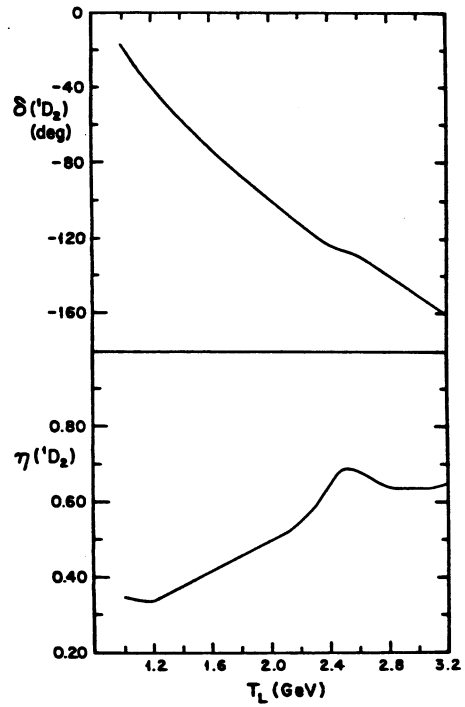

Fig. 4: The higher energy phase parameters for the $^1D_2$ model with CBM dynamics. The $NN(^1D_2)$ channel is coupled to $N\Delta(^5S_2)$, $N\Delta(^5D_2)$, $NN^*(^1D_2)$ and $\Delta\Delta(^5S_2)$. The boundary is $r_0^{\rm CBM} = 1.05$ fm and $W_p = 2.88$ GeV. The f-matrix elements are $f_{NN,NN} = 5.45$, $f_{N\Delta(S),N\Delta(S)} = 2.4$, $f_{N\Delta(D),N\Delta(D)} = 2.3$, $f_{NN^*,NN^*} = 0$, $f_{\Delta\Delta,\Delta\Delta} = 1.0$, $f_{NN,N\Delta(S)} = -1.6$, $f_{NN,N\Delta(D)} = 2.33$ and all other f-matrix components vanish. The potential matrix is described in the text.

to the $^1S_0$ described below. The amplitude estimate is, however, sensitive to details of the fit to the data at $T_L < 1$ GeV. Furthermore, the extrapolation of the background phases is also more model sensitive than in the $^1S_0$ case because of the higher energy. For these reasons, we postpone a detailed prediction of observable consequences of this resonance until the models are better determined.

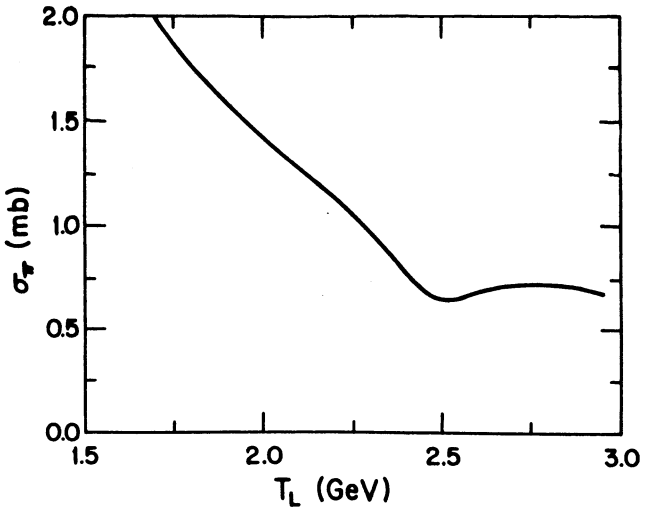

Fig. 5: One-pion production from the $NN(^1D_2)$ model described in Fig. 4, through the $N\Delta(^5S_2)$ and $N\Delta(^5D_2)$ channels.

III. CONSEQUENCES BETWEEN PP DATA AND THE $^1S_0$ STRUCTURE

In seeking correlations between our six-quark structure predictions and data it is important to keep in mind the relative sensitivity of different aspects of the predictions to uncertainties in the model. The widths and inelasticities of the resonances are determined by the fractional parentage coefficients of the six-quark configuration. This implies model independent results for the lower lying states in which configuration mixing is expected to be unimportant. In particular, for the lowest $^1S_0$ and $^3S_1$ resonances the width is predicted to be close to 50 MeV, and the $\Delta\Delta$ channel is expected to have a partial width almost equal to the elastic width.[4] We note here that the mass difference between the $^1S_0$ and $^3S_1$ resonances is determined by the color magnetic splitting, which, for every quark model, is adjusted to the N-Δ splitting. Hence, the prediction that the $^3S_1$ resonance is 70 MeV/c^2 lighter than the $^1S_0$ resonance is insensitive to the model.[4]

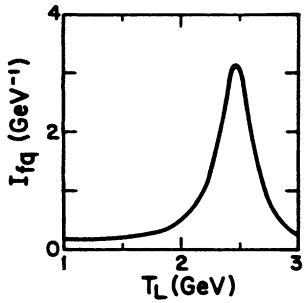

Fig. 6: The free-quark content, I_{fq}, of the $NN(^1D_2)$ coupled channel system with f-matrix pole determined by the Cloudy Bag Model.

The absolute position of the resonance is determined by the quark model used in the interior and by the boundary radius r_0. The latter is strongly restricted [Eq. (4)] by the same model but its precise value is determined by extrapolation of the experimental f-pole to its crossing with the quark state mass. For the CBM $^1S_0$ prediction [see Fig. 2(1) or Ref. 4a(b)] is uncertain by approximately ± 0.02 fm, leading to a change in barycentric mass of ± 25 MeV. The CBM itself is a good candidate on the basis of its success for hadron spectra as well as its reasonable success in fitting the lower energy two-nucleon data. But a small modification of the CBM, such as the inclusion of a quark self-energy term, may improve its fit to the hadron and two-nucleon data while shifting the six-quark resonance mass by the order of 25 MeV/c^2 (in addition to the shift due to the uncertainty of r_0).

The amplitude of the resonance is sensitive not only to the residue of the f-matrix pole (which is model insensitive) but also to the background amplitude of the resonating partial wave. The latter is sensitive to the detailed fit to the data for $T_L < 1$ GeV, via the constant f-matrix terms and parameterized two-pion exchange potentials. This is also true for the non resonating partial waves whose interference with the resonating partial wave determines the details of the angular distributions. The extrapolation of these backgrounds from $T_L = 1$ GeV to 2 GeV is affected not only by the uncertainties in the lower energy data, but also by the neglect in the model of isobar channel thresholds at higher energies than that of the $\Delta\Delta$ at $T_L = 1.4$ GeV.

Consequently, as mentioned in Section II(A), for our predictions we present the results of using two $^1S_0$ channel models, the best model (in terms of physics and fit) described above (NS) and the older version of Refs. [4] (OS) which may be more appropriate at $T_L = 2$ GeV when the higher thresholds are coupled.

For the partial waves other than the $^1S_0$ we use, for all observables studied, the recent full model results of Ref. [6] (NB). To show the sensitivity to the model used, we occasionally compare with the results of using the background partial waves of Refs. [4] (OB).

Below, we see that the data is consistent with the width and inelasticity of our predicted structure; that the energy of the predicted structure is about correct or up to 20 MeV/c^2 lower than the experimental result; and that the background phase shifts need to be shifted enough to move angular peaks by about 8°.

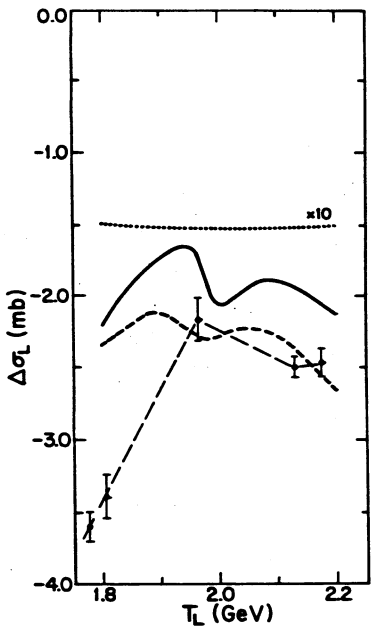

Fig. 7: The spin-dependent total cross section $\Delta\sigma_L$ in the region of the $^1S_0$ six-quark resonance, for pp scattering. The solid curve represents the OS,NB model and the dashed curve the NS,NB model, described in the text. The dotted curve is a result of extrapolating phases from the SAID solution (Ref. [12]). The filled circles are Argonne data points from Ref. [1] and the triangle is a CERN data point listed in Ref. [12]. The light long-dashed line is only to guide the eye.

A. $\Delta\sigma_L$ DATA

The most recent results[1] of the ZGS polarized proton beam-polarized hydrogen target data, in conjunction with previous data, reveals a maximum in $\Delta\sigma_L$ near T_L = 1.97 GeV followed by a minimum between 2.00 and 2.05 GeV. As shown in Fig. 7, the predictions for both OS and NS (with NB background) have the structure of a maximum followed by a minimum and a lesser maximum. In particular, for OS (the $^1S_0$ of Refs. [4]) the maximum is at T_L = 1.95 GeV and the minimum is at 2.02 GeV. The minimum is the effect of the six-quark resonance peak which produces a minimum in $\eta(^1S_0)$ as in Fig. 2 (or Fig. 2 in Ref. [4b]). The OS model amplitude, $\Delta\sigma_L(\text{max}) - \Delta\sigma_L(\text{min}) = 0.4$, is in agreement with that indicated by the data.

The gap in experimental data on either side of 1.97 GeV prevents an accurate determination of the positions of the maximum and minimum and only gives an upper limit of 80 MeV/c^2 for the width. The 50 MeV/c^2 predicted model widths are compatible, while the position of OS is either compatible with the data or low by no more than 45 MeV (15 MeV/c^2 mass). The NS model position is about 300 MeV low and its amplitude is only about half of the experimental result. Our background value of $\Delta\sigma_L$ has the correct sign but in OS is smaller in magnitude than the data by only 15%, while the NS "fits" the data (we note that the extrapolated phases of Arndt *et al.*[12] predict a $\Delta\sigma_L$ an order of magnitude too large).

B. C_{LL} DATA

Hint of a structure near T_L = 2 GeV was previously noted in C_{LL} data.[2] In Ref. [2], the discussion was concentrated on the 90° c.m. values because of the simpler phase shift structure. However, we note that the effects are stronger and more characteristic in the 50° – 75° range. Figure 8 shows the angular distribution of the data at two energies and of the OS, NB model for the three energies in the resonance region. The model predicts a maximum near 58°, while the data has a maximum at 68° (in the T_L = 1.967 GeV data there is one deviant point, producing a second maximum at 72°, for which we have no analog). By itself, this is not very indicative, but we also note a correspondence of model to data in the changing energy dependence below, at and above the angular peak. It is evident in Fig. 8 that, for both the model and the data below their angular peak C_{LL} increases with energy, above the angular peak it decreases with energy, while at the angular peak there is an energy peak at resonance.

This is clearly exhibited in the excitation functions $C_{LL}(T_L)$ of Fig. 9, which also includes T_L = 2.44 GeV data. The experimental statistical errors are two large and the energies too sparse to establish the details of a 50 MeV width structure; but the 63° and 66° experimental points increase with energy, the 69° points have a peak near T_L = 2.1 GeV and the 72° and 75° points decrease with the energy. Taking into account the 8° shift of the experimental peak for OS, NB, the situation is analogous for that model. The 54° excitation curve rises strongly from T_L = 1.8 GeV to 2.2 GeV (we do not extrapolate our model further because of the growing uncertainty), the 57° curve (near the angular peak) has a distinct maximum at T_L = 1.99 GeV and the 63° curve decreases strongly with energy. The absolute values of C_{LL} are consistent with the experimental results. The 54° and 63° curves have local maxima which would not be manifest in the widely spaced energies of the data. For comparison, Fig. 9 shows the predictions of the NS, NB model which has analogous variation with angle (the model angular peak is at 54°) of the broad energy behavior. The small bump-dip structure of the resonance, however, contrasts with the larger bump structure for the OS, NB model.

The C_{LL} (90°) situation is much less satisfactory in both the data and the model, as shown in Fig. 10. The data is consistent with a smooth behavior for 1.8 GeV < T_L < 2.7 GeV, although there is a hint of a knee between T_L = 2.13 GeV and 2.44 GeV. All four models arising from the choice of OS or NS and of OB or NB show a knee structure near T_L = 1.98 GeV which the current data is inadequate to exhibit. The models have a slope consistent with that of the data, but are much more negative in value. It is likely that the model is not only unreliable for the background value

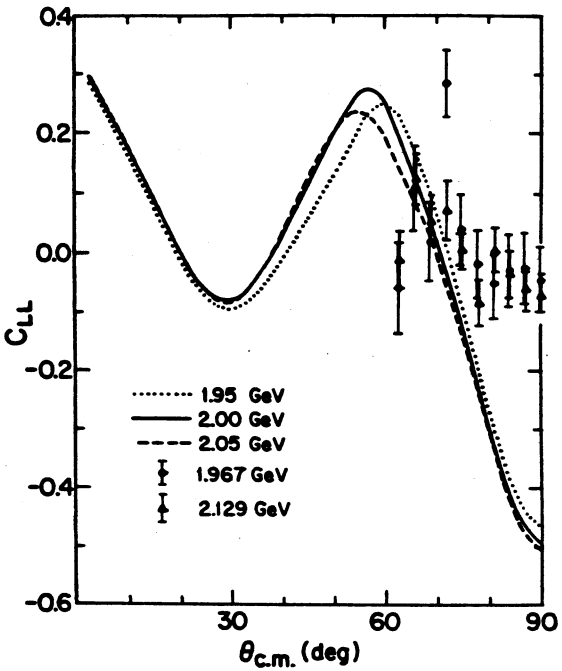

Fig. 8: C_{LL} angular distributions for energies near the $^1S_0$ resonance and for the OS,NB model. The experimental points are those of Ref. [2].

near 90°, but also for the structure which is mostly a reflection of the structure of $d\sigma/d\Omega$ (90°), *i.e.* it does not appear strongly in $C_{LL}d\sigma/d\Omega$ which is bilinear in the amplitudes. The model production for $d\sigma/d\Omega$ qualitatively agree with the data for $\theta < 70°$. However, for $70° < \theta < 90°$ the data continues its monotonic decrease but the models predict a rise to a small maximum at 90°. This implies that the singlet (even) partial waves with $L \geq 4$ (for which the coupled channel models have not been developed[6,7]) are inadequately represented but are important at this energy. The 90° predictions of the model can only be considered to give an indication of the width and amplitude of the structure.

C. C_{NN} DATA

The possibility of experimental structure in C_{NN} (90°) near $T_L = 2$ GeV has previously been noted.[3] Figure 11 shows that our models are consistent in slope with the 90° data (and that the OS, NB and NS, OB models are close in value) but that

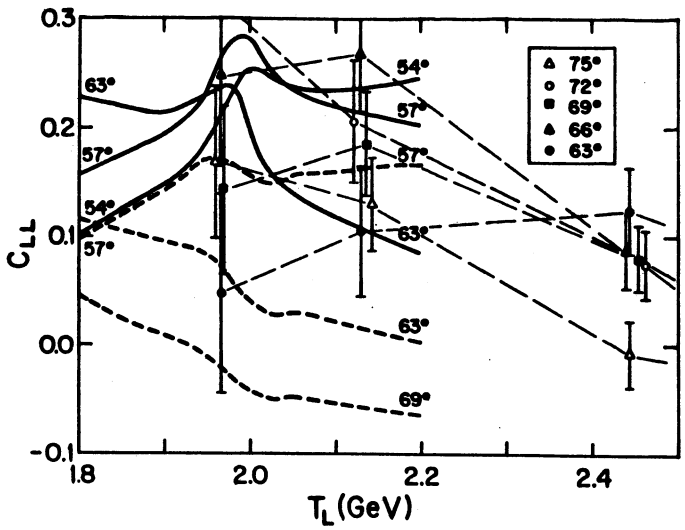

Fig. 9: A few C_{LL} excitation functions at sensitive angles for $1.8 < T_L < 2.2$ GeV. The curves for model predictions are as in Fig. 7. The three sets of experimental points (Ref. [2]) are precisely at $T_L = 1.967$, 2.129 and 2.444 GeV (in each set, points have been slightly separated to distinguish them).

the data energy steps are much too large to discern the predicted structure. We note that the amplitude of the structure predicted by OS, NB model, favored by $\Delta\sigma_L$ and C_{LL} data, is quite large.

As in the case of C_{LL}, it turns out that the best evidence of compatibility of our model for C_{NN} is in the angular distribution near the resonance energy. The data at $T_L = 1.97$ GeV is compared with the OS, NB model in Fig. 12. The slope and the absolute values match well if one allows for a shift of 7° of the first minimum below 90° (62° in the data, 69° in the model). This gives some confidence to our energy dependence predictions near 60° (to be applied to 67° data). Indeed, a well-marked dip-bump structure is predicted for this angle, as shown in Fig. 13. This figure also displays predictions for $\theta = 48°$, 63° and 69°, and for the NS, NB model at 63° and 69°.

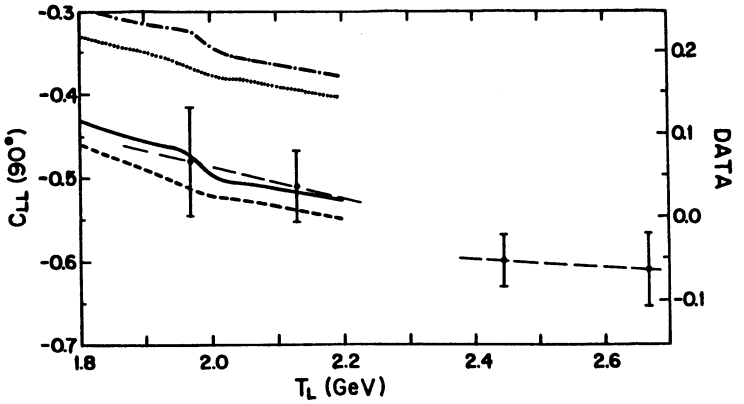

Fig. 10: The energy dependence of C_{LL} (90°). The solid curve represents the OS,NB model; the dashed curve the NS,NB model; the dash-dotted curve the OS,OB model and the dotted curve the NS,OB model, described in the text. The last plotted data point is at $T_L = 2.666$ GeV (Ref. [2]).

D. OTHER OBSERVABLES

As shown in Fig. 14, any combination of models predicts a structure in $\Delta\sigma_T$ and the amplitude of the structure for the OS, NB model is large. There have recently been extensive measurements[15] of $\Delta\sigma_T$ up to $T_L = 3$ GeV, but unfortunately there is no measurement between $T_L = 1.8$ GeV and 2.1 GeV. At those energies the NB models agree with the sign of the data, but are an order of magnitude too big. The OB models give the magnitude of the background.

There are measurements of P at several angles for $T_L = 1.968$ GeV as partly shown in Fig. 15. It is possible that measurements of P, D and D_t can be made at the Saturne synchrotron with a gas jet target in the polarized beam in the angular range $60° < \theta_{cm} < 120°$. This has the advantage of providing accurate measurements at every 5 or 6 MeV [16] so that many of the structures indicated in Fig. 15 such as $P(63°)$, $D(60°, 69°, 90°)$ and $D_t(39°, 45°, 57°, 63°)$ would be observable.[17] It is indeed possible at these energies to attain a precision of $\Delta P \sim .01$ and $\Delta D \sim .03$ (allowing longer energy steps and data taking time).

The appearance of the structure in other spin observables (A, A', R, R', A_{XX}) at sensitive angles is shown in Fig. 16 for the OS, NB model.

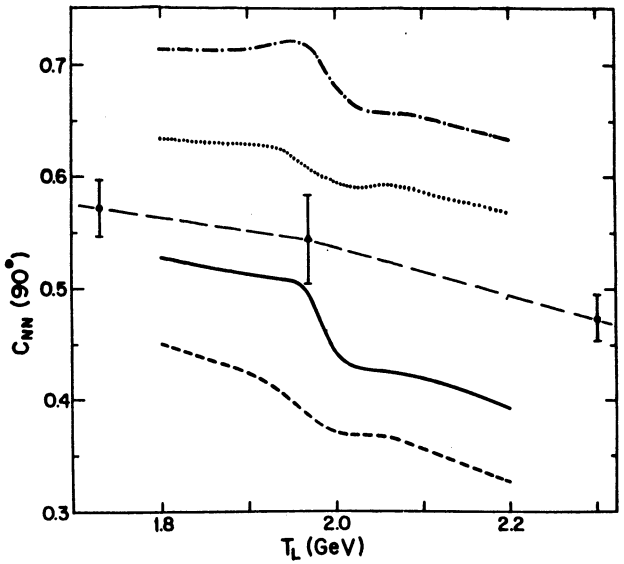

Fig. 11: The energy dependence of C_{NN} (90°) for $1.8 < T_L < 2.2$ GeV. The curves for model predictions are as in Fig. 10. The filled circles are from Ref. [3a] and the triangle is from Ref. [3b].

IV. CONCLUSIONS

We have shown that the coupled channel model including isobar width effects and interior CBM dynamics can successfully fit the $^1S_0$ and $^1D_2$ nucleon-nucleon scattering data (and two-pion production) for $T_L < 1$ GeV. In the $^1D_2$ case, there is more ambiguity in the choice of r_0 than in the $^1S_0$ case due to the greater extrapolation in energy needed for the experimental f-matrix pole. We have chosen the same r_0 for both channels.

The extrapolation of the model phase shifts to higher energies shows small NN^* and $\Delta\Delta$ threshold structures and substantial structures at the six-quark resonance positions for both the $^1S_0$ and $^1D_2$ channels. The width of the predicted $^1D_2$ structure is about twice that of the 50 MeV/c^2 $^1S_0$ structure width. The splitting of the $^1D_2$ from the $^1S_0$ structure is uncertain due to the relatively large uncertainty in $r_0^{\rm CBM}$ for the higher energy $^1D_2$ case. It can be from about 30 MeV/c^2 to 170 MeV/c^2 higher in mass. With our present choice $r_0^{\rm CBM} = 1.05$ fm, $M(^1S_0) = 2.71$ GeV/c^2 ($T_L = 2.04$ GeV) and $M(^1D_2) = 2.88$ GeV/c^2 ($T_L = 2.54$ GeV). The resonances are centered at slightly lower values of T_L (by about 35 MeV) because of the coupled channel effects[4] on the nucleon-nucleon channel.

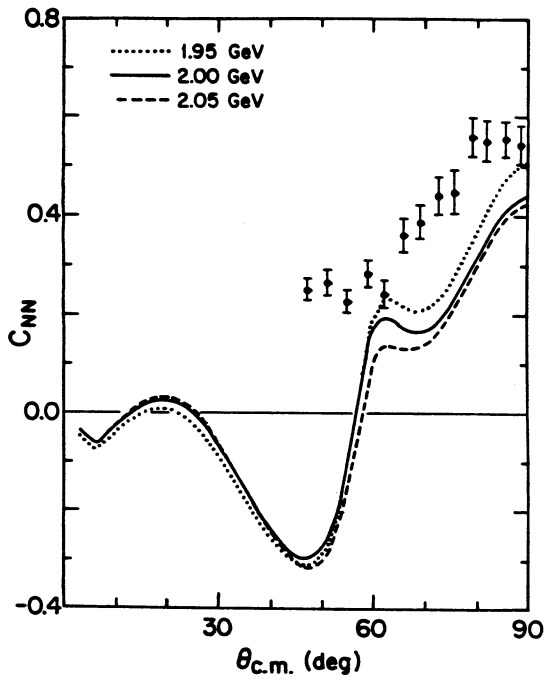

Fig. 12: C_{NN} angular distributions for energies near the $^1S_0$ resonance and for the OS,NB model. The data points at $T_L = 1.968$ GeV are those of Ref. [3b].

In the present article we have examined the consequences of the $^1S_0$ structure for many spin observables in the $T_L = 1.8$ GeV to 2.2 GeV region. We postpone such detailed predictions of the observable consequences of the $^1D_2$ structure because of the greater uncertainty of its parameters. It is possible that the $^1D_2$ structure may be centered as low as $T_L = 2.15$ GeV, but the data we have examined gives no indication that this is so. The knee that may be present in the C_{LL} (90°) excitation curve between $T_L = 2.13$ GeV and 2.44 GeV could be a consequence of the $^1D_2$ structure. In the near future, we intend to examine the observable consequences of the $^1D_2$ state, after having better determined the model by using the non-resonant data for $T_L = 1-3$ GeV.

We have compared in detail the observable consequences of the $^1S_0$ six-quark structure with experiment results in the resonance region. Both the $^1S_0$ model discussed above and an older version[4] were used for comparison. For the other phase shifts the best available models of Ref. [6] were used, but occasional comparisons with the results of older models[4,7] were made to indicate sensitivity.

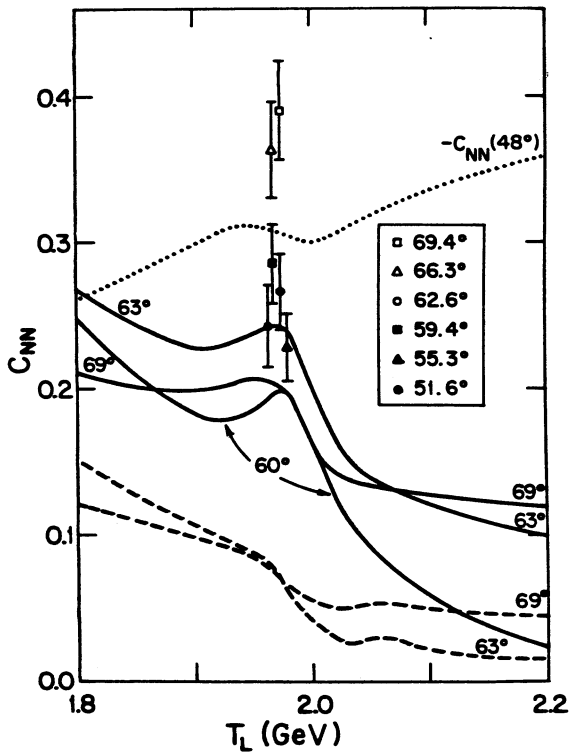

Fig. 13: A few C_{NN} excitation functions at sensitive angles and a few data points all at $T_L = 1.968$ GeV (Ref. [3b]). Except for the dotted curve which is $-C_{NN}$ (48°), the curves are as in Fig. 7.

The recently observed[1] bump-dip structure in $\Delta\sigma_L$ corresponds well to the predictions of the OS, NB model (the NS, NB structure is similar but is of smaller amplitude). The experimental energy points are too far apart to precisely verify either the energy position or width. Our width of 50 MeV/c^2 is consistent with the experimental upper limit of 80 MeV/c^2. The experimental energy of the structure corresponds to our predicted mass or up to 15 MeV/c^2 higher.

The experimental behavior of $C_{LL}(\theta)$ in the energy region is also similar to the OS, NB prediction. Allowing for a shift of 8° in the angular peak, there is a strong correspondence of the non-trivial variation in energy dependence from below to above the angular peak. The energy peak in the data is consistent with the mass of our resonance, but is also consistent with a mass of up to 50 MeV/c^2 higher. The data

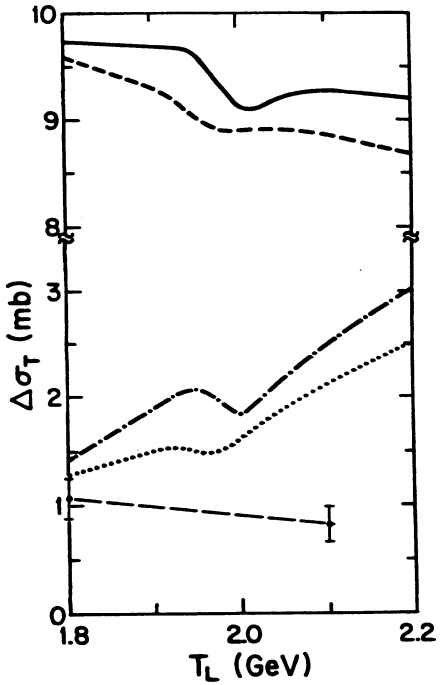

Fig. 14: The spin-dependent total cross section $\Delta\sigma_T$ in the region of the $^1S_0$ six-quark resonance. The curves represent the four models identified in Fig. 10. Data points are from Ref. [15].

at 90° is not inconsistent with our energy dependence, but does not have sufficient resolution to compare with the structure. Further, our model is poor at 90° with respect to the background values of both C_{LL} and $d\sigma/d\Omega$.

The experimental $C_{NN}(\theta)$ at $T_L = 1.97$ GeV corresponds closely to our predictions, allowing for a 7° of the first minimum below 90°. We predict substantial energy dependence near 60° as well as at 90°. Only at 90° is there data at several energies in the vicinity. The data is consistent with our predicted energy dependence, but the experimental energies are too far apart for a meaningful comparison with the structure.

We have also predicted that measurable structures are present in $\Delta\sigma_T$, P, D, D_t, A, A', R, R' and A_{XX}. Although we have presented some tantalizing evidence that the data may support the existence of a structure with the characteristics of our

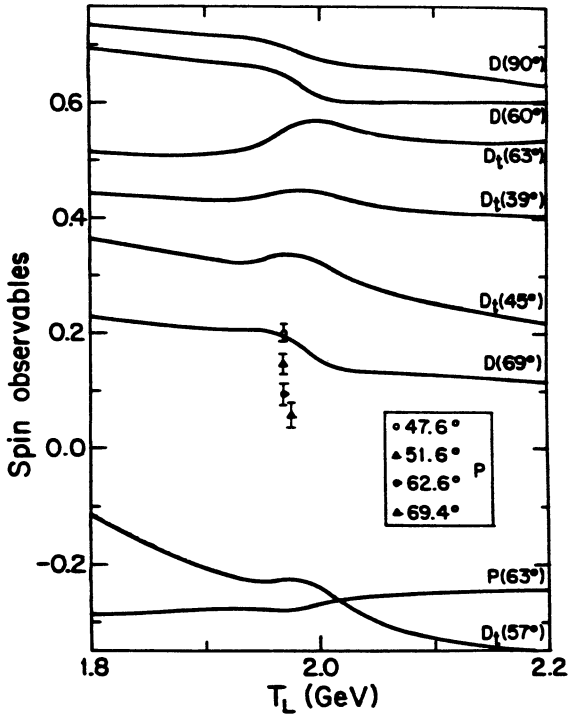

Fig. 15: Energy dependences of the polarization P, depolarization D and polarization transfer D_t at several sensitive angles. All the curves are for the OS,NB model. For pp scattering $D(\theta) = D_t(\pi - \theta)$. The experimental points for P are all at $T_L = 1.968$ GeV (Ref. [3b]) and indicate the magnitude of the background.

predicted $^1S_0$ six-quark resonance, it is clear that more data is required to verify such an assertion. More precise data on $\Delta\sigma_L$, C_{LL} and C_{NN} at several energies close to $T_L = 2$ GeV is likely to be definitive. But other observables, such as $\Delta\sigma_T$, P, D, and D_t may be feasible with the required precision and energy step size. We note that the position of the resonance depends on the quark model and that plausible variations in that model may shift the position of the resonance by the order of 100 MeV/c^2 Thus, whether the structure is where indicated by the present $\Delta\sigma_L$ data[1] or turns up elsewhere, it will be important to verify the less model sensitive characteristics of width and inelasticity.

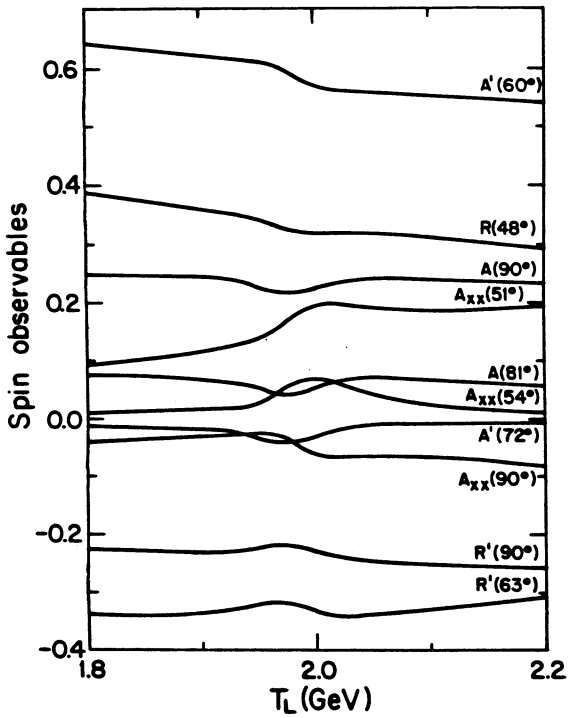

Fig. 16: Choices among the subset of pp polarization observables A, A', R, R' and A_{XX} whose excitation functions feature the six-quark resonance. All the curves are for the OS,NB model. There is no data in this energy region.

Because of its sensitivity to the particular quark or hadron force model, a particularly important verification of the six-quark resonance nature would be the discovery of a $^3S_1$ resonance 70 MeV/c^2 lower in mass than the $^1S_0$. Experiments in the np system for $T_L = 1.8$ GeV are highly desirable.[4] In the pp system there is similar interest in the examination of the $T_L = 2.0 - 2.6$ GeV region for a $^1D_2$ structure, but the energy spacing is less well-predicted.

There are also needed improvements in the model. Although the data for $T_L > 1$ GeV is not extensive enough for a phase shift analysis, we intend to improve our hadron models by directly fitting the available background data. This may require the coupling of additional isobar channels of higher threshold energy. We also intend to

investigate the effects of modifying the CBM by the addition of a quark self-energy term.

ACKNOWLEDGEMENTS

We are grateful to Prof. A. Yokasawa for early communication of his recent $\Delta\sigma_L$ results and to Dr. M. Garçon for his information on experimental possibilities. In the course of this work, one of us (E.L.L.) benefited from the hospitality and facilities of the Physics Division of Los Alamos National Laboratory. P.L.F. is grateful for the support provided by the Natural Sciences and Engineering Research Council of Canada and the warm hospitality of the Center for Theoretical Physics at MIT, and P. G. for the support provided by the Fulbright program.

REFERENCES

1. I. P. Auer *et al.*, preprint ANL-HEP-PR-86, submitted to *Phys. Rev. Lett.*
2. I. P. Auer *et al.*, *Phys. Rev. Lett.* **48**, 1150 (1982).
3. (a) A. Lin *et al.*, *Phys. Lett.* **74B**, 273 (1978); (b) Bell *et al.*, *Phys. Lett.* **94B**, 310 (1980).
4. (a) E. L. Lomon, *Nucl. Phys.* **A434**, 139c (1985); (b) P. LaFrance and E. L. Lomon, to be published in *Phys. Rev.* **D**.
5. A. W. Thomas, S. Théberge and G. A. Miller, *Phys. Rev.* **D24**, 216 (1981); P. J. Mulders and A. W. Thomas, *J. Phys.* **G9**, 1159 (1983).
6. P. González and E. L. Lomon, to be published in *Phys. Rev.* **D**.
7. E. L. Lomon, *Phys. Rev.* **D26**, 576 (1982).
8. E. L. Lomon and H. Feshbach, *Ann. Phys.* (N.Y.) **48**, 94 (1968).
9. F. H. Cverna *et al.*, *Phys. Rev.* **C23**, 1698 (1981).
10. Joseph A. Minahan, MIT thesis (for B.Sc. degree) June 1982.
11. D. B. Bugg, private communication.
12. R. A Arndt *et al.*, *Phys. Rev.* **D28**, 97 (1983) and FALL 85 SAID Solution.
13. M. Harvey, *Nucl. Phys.* **A352**, 301 (1981), see Table II.
14. E. L. Lomon, *Phys. Rev.* **D1**, 549 (1970).
15. F. Perrot *et al.*, preprint CEN-Saclay DPhPE/April 86.
16. M. Garçon *et al.*, *Nucl. Phys.* **A445**, 669 (1985).
17. M. Garçon, private communication.